Turkish Journal of Electrical Engineering & Computer Sciences

http://journals.tubitak.gov.tr/elektrik/

Research Article

Turk J Elec Eng & Comp Sci
(2017) 25: 4242 – 4253

doi:10.3906/elk-1612-336

Sphere decoding algorithm for multiuser detection in a distributed antenna system

Fahad KHAWAJA*, **Alam ZAIB**, **Shahid KHATTAK**
Department of Electrical Engineering, Faculty of Engineering, COMSATS Institute of Information Technology, Abbottabad, Pakistan

Received: 28.12.2016 • **Accepted/Published Online:** 03.05.2017 • **Final Version:** 05.10.2017

Abstract: In this paper, the impact of initial search radius on the complexity and performance of a sphere decoding algorithm is investigated for different user positions within a distributed antenna system. In a distributed antenna system, users can take up random positions within the cell clusters. The channel matrix can therefore take up infinitely different forms. In the presented work, a distributed antenna system with three different user positions in the cooperating cells is considered by employing different channel matrices. The effect on the complexity and performance of the sphere decoder due to the choice of the initial sphere radius is investigated for these user positions. It is shown that the signal lattice volume changes considerably for different user positions within the cells. A dynamic radius allocation algorithm is proposed in which the behavior is exploited by dynamically adjusting the initial sphere radius based on the knowledge of the channel path gain matrix. The simulation results show that the proposed algorithm results in a considerable reduction in the complexity of the sphere decoder in a distributed antenna system. Additionally, the performance of the sphere decoder in different coupling scenarios within the distributed antenna system has been investigated for a different number of candidates. It is shown that the performance of cell edge users can be considerably enhanced with high channel diversity, which otherwise could severely deteriorate the overall system performance.

Key words: Sphere decoding, distributed antenna system, sphere radius, multiuser detection

1. Introduction

In the last few decades, there has been a rapid increase in the information transmission rate due to the unprecedented usage of wireless devices, and the trend is expected to continue in the future. Modern-day wireless communication systems are therefore required to deliver high performance at a low complexity while operating at a high data rate. An elegant way to improve the data rate and/or the spectral efficiency of wireless communication systems is to use a distributed antenna system (DAS). In a DAS, the intercell interference is eliminated through joint detection, which results in improved system performance. The cochannel signals received by the neighboring base stations (BSs) are sent to a single central point for joint processing and detection of multiuser signals. This arrangement forms a virtual multiple-input multiple-output (MIMO) system where the strength of the received signal may vary depending upon the position of the users within the cells. Hence, the performance of the users at the cell edges can be greatly improved, thereby boosting the quality of service in the entire cell [1].

DAS have been shown to be very effective in reducing intercell interference and eliminating dead spots

*Correspondence: fahadmasood@ciit.net.pk

[2]. To utilize the advantages offered by a DAS, different linear and iterative receivers have been implemented for multiuser detection (MUD). In [3], linear schemes such as zero forcing (ZF) and minimum mean square error (MMSE) are implemented, but these schemes do not offer the desired bit error rate (BER) performance. In [4], multiuser turbo detection in a DAS was implemented using linear filters for initial detection. More complex receiver strategies like successive interference cancellation (SIC) and parallel interference cancelation have also been investigated for a DAS in [5]. All these schemes either have a lower diversity or suffer from an error propagation that results in a significant performance loss. High performing optimum detection techniques such as ML and maximum a posteriori have not been considered for a DAS due to their prohibitively large complexity.

For MIMO systems, the main challenge is to perform joint data detection with reduced complexity at the receiver. In this regard, sphere decoding (SD) has shown some promising results and is capable of providing near optimal performance approaching that of a maximum likelihood (ML) receiver but at much lower complexity [6]. The key idea in SD is that the search for the transmitted signal vector is limited to a sphere of a certain radius instead of the whole signal lattice, thereby reducing the computational complexity.

Because of its computational advantages over ML, SD has attracted a lot of interest in the research community. The concept of the SD algorithm was initially proposed by Phost in [7], which formulated the data-detection problem as solving the closest lattice problem. Subsequent improvements were made thereafter, e.g., in [8–12], in order to apply SD to MIMO systems and to reduce the search complexity of the SD algorithm. In [13], the concept of ordering the layers according to signal-to-noise-ratio (SNR) was used in a sorted QR decomposition along with MMSE filtering. Here, the complexity and the error propagation were reduced by layer ordering as the strongest SNR layers were being searched first. In [14], SD with different preprocessing schemes was compared, and it was shown that SD with MMSE filtering and layer ordering gave the best performance that closely approached that of the ML receiver. The complexity of the SD algorithm is known to be highly dependent on the initial search radius. In [15], SD with reduced complexity was proposed, in which the search radius of the SD algorithm was dynamically updated using the largest value among the Euclidian distance of detected candidates. Another approach based on SIC was used in [16], which aids in tree pruning to further reduce the complexity of the SD algorithm.

Although SD has been extensively investigated for MIMO systems, its behavior in a DAS has yet to be explored. The relationship between the complexity of SD receivers and the shape of the channel matrices encountered in a DAS and the resulting optimal choice of the initial sphere radius merits additional study. This has motivated us to investigate the selection of the initial sphere radius and the impact of different user positions within a cell on the complexity and performance of SD for MUD in a DAS.

In this paper, SD is implemented for MUD in a DAS. A framework for investigating the performance of the cooperating communication system is developed in order to yield meaningful results. The effect of different users' positions on the performance of the receiver and the sphere radius is investigated. It is shown that SD receivers give a performance close to ML receivers for different users' positions within a cell. The search complexity of the SD can be reduced with an appropriate selection of the initial search radius, as shown in [17]. However, a fixed value of the initial radius will increase the search complexity. Therefore, the initial sphere radius is evaluated for different users' positions within the cooperating cells in order to reduce the number of candidates. It is shown that the number of visited nodes and hence the complexity are reduced when the initial sphere radius is dynamically updated using the volume of the received signal lattice.

The remainder of this paper is organized into the following sections. In Section 2, the problem framework

is laid out, which includes the system model and the receiver block diagram. In Section 3, the SD algorithm for a DAS is explained. The effect of the channel path gain matrix on the sphere radius is discussed in Section 4, and conclusions are drawn in Section 5.

2. The problem framework

2.1. System model

In this article, an uplink OFDM transmission in a DAS is considered with N_R cooperating cells, each with a single antenna BS. The DAS contains N_T single antenna cochannel mobile terminals (MT), where $N_T \leq N_R$. The MT signal is not only received by its own BS but also by the BSs in the neighboring cells. The baseband received system model for the mth subcarrier is given as:

$$\mathbf{y}_m = \mathbf{H}_m \mathbf{x}_m + \mathbf{n}_m, \tag{1}$$

where the channel matrix $\mathbf{H}_m$ has complex Gaussian random entries $\mathbf{H}_m \in C^{[N_R \times N_T]}$. The transmit symbol vector $\mathbf{x}_m$ is a complex uniformly distributed random vector $\mathbf{x}_m \in C^{[N_T \times 1]}$ such that its elements $x_i \in A$, where A is the modulation alphabet of size $|A| = M$ The received signal vector is $\mathbf{y}_m \in C^{[N_R \times 1]}$, and the noise vector $\mathbf{n}_m$ is a zero mean circularly symmetric Gaussian random vector having covariance matrix $\sigma^2_{n_m}\mathbf{I}$, i.e. $\mathbf{n}_m \in C^{[N_R \times 1]}[\mathbf{0}, \sigma^2_{n_m}\mathbf{I}]$, where $\mathbf{0}$ is a vector of all zero elements, and $\mathbf{I}$ is an identity matrix. Since OFDM eliminates the interference between subcarriers, the processing for each subcarrier is done independently of the others. For this reason and for notational convenience, the subcarrier index m will be omitted in the remainder of this article.

The channel matrix $\mathbf{H}$ in a DAS can be written as $\mathbf{H} = \mathbf{G} \odot \mathbf{H}'$. Here, $\mathbf{H}'$ represents the small-scale fading behavior of the selected channel and is called the channel model matrix. $\mathbf{G}$ represents the relative signal strength due to variable path gains resulting from different users' positions within the cooperating cells and is called the channel path gain matrix. The operator $\odot$ represents an element-wise multiplication. Assuming closed-loop power control with respect to the local BS of each MT, the channel path gain matrix can be written as [18]:

$$\mathbf{G} = E_s/N_0 \begin{bmatrix} 1 & \rho_{12} & \cdots & \rho_{1N_T} \\ \rho_{21} & 1 & \cdots & \rho_{2N_T} \\ \vdots & \vdots & \ddots & \vdots \\ \rho_{N_R1} & \rho_{N_R2} & \cdots & 1 \end{bmatrix}, \tag{2}$$

where E_s/N_0 is the SNR maintained with respect to the local BS. The diagonal entries of matrix ρ_{ii} represent the path gain between the ith MT and the associated ith BS, and the nondiagonal entries ρ_{ij} represent the path gain between the ith MT and jth BS, whose values would normally reside between 0 and 1 based on the MT's position [18]. Since there can be infinitely different realizations, only the more comprehensible symmetric scenarios are considered here for which all the nondiagonal entries are equal. $\rho_{ij} = \rho$, i.e.:

$$\mathbf{G} = E_s/N_0 \begin{bmatrix} 1 & \rho & \rho & \rho \\ \rho & 1 & \rho & \rho \\ \vdots & \vdots & \ddots & \vdots \\ \rho & \rho & \cdots & 1 \end{bmatrix}, \text{where } 0 \leq \rho \leq 1. \tag{3}$$

As ρ changes from 0 to 1, the MTs are expected to move from under the BS towards the cell boundary. In this paper, only three different cases of the relative user positions are investigated. In the first scenario, all the MTs are clustered at the common cell boundary and can be considered at the same distance from all of the BSs. This scenario has been referred to as fully coupled (FC) with $\rho = 1$. In the second scenario, the MTs reside in the interior of the cells, but the transmit signal is still strong enough to be received by the neighboring BSs. This scenario has been referred to as partially coupled (PC) with $\rho = 1/2$. In the third scenario, all of the MTs in each cell are very close to the local BS, and this scenario has been referred to as isolated (ISO) since the MT transmit power is so low that no signal is effectively received by the neighboring BS, i.e. $\rho = 0$. Figure 1 shows a 4-cell system, each with a BS. The paths taken by the MT in each cell, as the coupling ρ varies from 0 to 1, are along the four arrowed lines all pointing to a common boundary point. The markers on these lines indicate the position of the MT for the three scenarios to be investigated. Coupling is negligible when the MT is close to the local BS and strongest when the MT is at the cell edge.

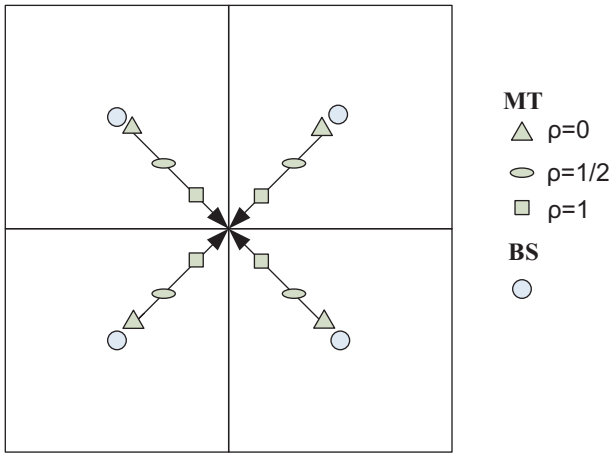

Figure 1. Four-cell DAS showing the approximate position of the MT within the cells as ρ changes from zero to one.

2.2. DAS receiver block diagram

Figure 2 shows the block diagram of the receiver where bit-interleaved coded modulation (BICM) data streams transmitted from N_T MTs are linearly superimposed at each of the N_R receive antennas of the BSs as signal r. Each BS only performs the radio frequency front-end processing, and the sampled base-band signal vector $\mathbf{y} = [y_1, y_2, y_3 \ldots y_{N_R}]^T$ is sent to the central processing point where the joint detection and decoding takes place. Here, SD is used for signal detection and its output estimate $\hat{v} = [\hat{v}_1, \hat{v}_2 \hat{v}_3 \ldots . \hat{v}_{N_R}]^T$ is then deinterleaved and sent to the soft-input soft-output turbo decoder.

3. Sphere decoding algorithm for a DAS

The SD receiver searches for the signal estimate from the constellation points that lie within a small sphere around the initial approximate guess within the signal lattice. Unlike the optimum ML detection, it avoids searching the complete signal lattice and therefore offers a near optimal performance at a much reduced complexity. The SD receiver searches to find the near optimal solution for all those hypotheses $\tilde{x}$ that satisfy:

$$\|\mathbf{y} - \mathbf{H}\tilde{x}\|^2 < d^2, \tag{4}$$

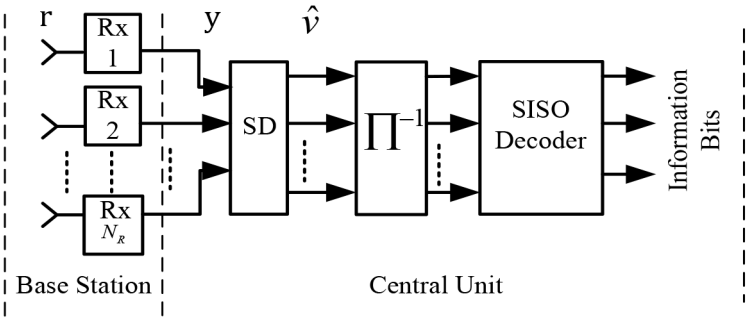

Figure 2. Block diagram of the SD receiver at the central processing point in a DAS.

where d is the initial radius of the sphere. The channel matrix can be decomposed as $\mathbf{H} = \mathbf{QR}$, where $\mathbf{Q}$ is a unitary matrix $\mathbf{Q}^H\mathbf{Q} = I$, and $\mathbf{R}$ is an upper triangular matrix with its diagonal terms arranged in ascending order. Now Eq. (4) can be written according to [14] as:

$$\|\mathbf{y} - \mathbf{QR}\tilde{x}\|^2 < d^2,$$

$$\left\|\mathbf{Q}^H\mathbf{y} - \mathbf{R}\tilde{x}\right\|^2 < d^2,$$

$$\|\mathbf{y}' - \mathbf{R}\tilde{x}\|^2 < d^2,$$

$$\Omega = \sum_{i=l}^{N_T} \left| y_i{}' - \sum_{j=i}^{N_T} r_{i,j}\tilde{x}_j \right|^2 < d^2, \qquad l = 1 \ldots N_T. \tag{5}$$

The SD algorithm starts at the last (N_T) layer, where the metric Ω is calculated, and then goes up to the first layer using back substitution. The initial value of search radius d is based on the channel conditions and the number of candidates required. This initial value is used for searching the lattice points in the first layer. At each layer, the Euclidean distance between the received symbol and the closest lattice point is evaluated and is then subtracted from the search radius value to give an updated, smaller search radius for the next layer. This process continues until the leaf node in the last layer is reached or the search radius diminishes to zero. The metric Ω for a specific candidate is generated by accumulating the Euclidian distance for all of the symbols. If the sphere radius is greater than the metric Ω of a given candidate, then the candidate is added to the list of candidates; otherwise, it is discarded. If the number of candidates found is less than the number of desired candidates, the initial value of the search radius d is increased by a factor α, and the entire search process is repeated. The search continues until the required number of candidates N_C is found. The value of α depends on the signal lattice dimensions and the probability density distribution of the determinant of the channel matrix. The best value of α is empirically determined by averaging the total number of node points visited in the search tree and, for a 4×4 MIMO system, its value normally lies between one and two, i.e. $1 \leq \alpha \leq 2$.

The complexity of SD strongly depends on the size of the initial search sphere. As the size of the sphere increases, the number of candidates within the sphere grows and the complexity increases. A higher number of candidates, however, increases the likelihood of finding the optimal solution with a consequent improvement in performance. If d is taken too large, the number of candidates or hypotheses within the sphere grows, which in turn increases the search complexity. Conversely, if d is very small, the number of candidates within the sphere

will be less than the desired number of candidates, and the search will restart again with an increased radius, thereby repeating the computational effort. In [19] and [20], the ZF estimate is used to set the initial sphere center. The ZF solution gives the Babai point [21]. If the Euclidian distance between the Babai point and the closest lattice point is taken as the search radius, at least one candidate lies within this search sphere. This, however, is not suitable if the number of candidates required is more than 1. A method of finding the sphere radius based on the statistics of the noise is given in [22] as:

$$\|\mathbf{y}-\mathbf{Hx}\|^2 = \|\mathbf{n}\|^2 \sim \sigma_n^2 \chi^2_{2N_R} \tag{6}$$

where $\chi^2_{2N_R}$ denotes a chi-square random variable having $2N_R$ degrees of freedom and a mean value of $E[\chi^2_{2N_R}] = 2N_R$. The sphere radius is now calculated as [22]:

$$d^2 = \sigma_n^2 2N_R K \tag{7}$$

The value of K is calculated using the equation from [22], $K = \frac{1}{60} qRc\sqrt{\frac{E_b}{N_0}}$, where q is the number of bits per symbol, Rc is the code rate, E_b is the energy per bit, and $N_0 = \sigma_n^2$. This will ensure that at least one candidate lies within the sphere. In order to have more than one candidate, the value of K can be empirically scaled.

The SD algorithm is explained in Table 1. The initial sphere radius d may be grown by a factor of α until the required number of candidates is found. The list of candidates generated at the output of SD is denoted by C.

Table 1. Sphere decoding algorithm.

Input: $d^2, N_C, \mathbf{R}, \mathbf{y}, \alpha$

Output: C

1) **while** $length(C) < N_C$
2) **for** $l = N_T \rightarrow 1$
3) $\Omega = \sum_{i=l}^{N_T} \left| y_i' - \sum_{j=i}^{N_T} r_{i,j} x_j \right|^2 < d^2$.
4) **end for**
5) C stores all $\Omega < d^2$
6) **if** length $(C) < N_C$
7) $d^2 = d^2 \times \alpha$
8) **end if**
9) **end while**

Table 2. Number of candidates visited for fixed versus adaptive initial radius; i.i.d. Rayleigh channel and 16 QAM.

E_b/N_0 [dB]			0	2	4	6	8
Fixed radius		Square of radius d^2	3	4.0	5.3	7.2	9.9
	Fully coupled	No. of candidates	14	24	31	36	40
	Partially coupled	No. of candidates	110	196	257	297	322
	Isolated	No. of candidates	453	915	1300	1605	1831
Adaptive radius	Fully coupled	Square of radius d^2	1.23	1.90	3.00	4.80	7.60
		No. of candidates	5.11	10.01	14.12	18.2	20.1
	Partially coupled	Square of radius d^2	0.56	0.90	1.42	2.25	3.60
		No. of candidates	6.32	11.21	16.24	21.1	25.3
	Isolated	Square of radius d^2	0.44	0.68	1.15	1.70	2.90
		No. of candidates	7.21	15.1	23.44	30.3	39.4

4. Effect of the channel path gain matrix on sphere radius

Any change in the MT position in the cooperating cells changes the coupling between the received signals of different users, which is reflected by the coefficients of channel gain matrix **G** and channel matrix **H**. For different realizations of **H**, the transmit signal lattice (a hypercube in $2N_T$ dimensional Euclidean space) is scaled differently along its different dimensions, and the resulting received signal lattice has different sizes. Thus, the number of candidates within a specific value of the initial sphere radius is different from one channel realization to another.

For the results presented in this section, we assume 16 QAM and independent and identically distributed (i.i.d.) Rayleigh channels. However, the conclusion obtained can easily be generalized to other scenarios. Figure 3 shows the average number of candidates for different values of the initial sphere radius normalized by the minimum spacing between the constellation points. For the three considered scenarios, FC, PC, and ISO, the number of candidates increases as the coupling between the MT and the BS decreases. For a specific normalized sphere radius of 1.6, the number of candidates for the FC scenario is around 20, for PC it is around 100, and for ISO it is around 800. This variation in the number of candidates is due the fact that the size of the signal lattice changes when channel matrix **H** is altered. In [23], the volume in which one candidate resides is given by $V_{unit}=a^L|\det\mathbf{H}|$, where a is the minimum spacing between adjacent lattice points, $L=2N_T$ is the number of real dimensions, and $\det\mathbf{H}$ represents the determinant of matrix **H**. The volume occupied by a single candidate depends on the determinant of the channel matrix **H** In order to explain how user position affects the lattice

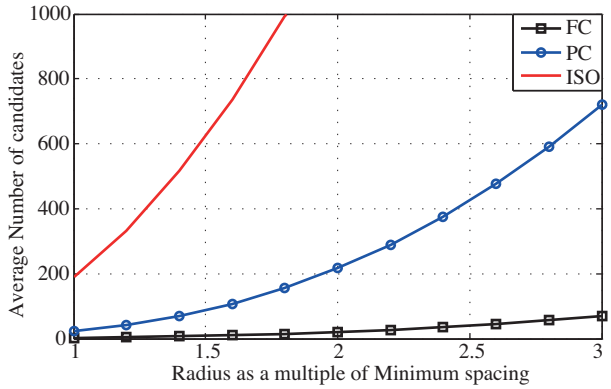

Figure 3. Average number of candidates versus initial sphere radius comparison.

size, the average values of $|\det\mathbf{H}|$ for the three considered scenarios of FC, PC, and ISO are 24.2, 1.6, and 1.1, respectively, at SNR= 4 dB. Thus, the lattice volume in which a single candidate resides decreases with the reduction in signal coupling. The number of candidates for a given value of the initial sphere radius d is therefore lowest for the FC scenario and highest for the ISO scenario, as shown in Figure 3. Having a fixed radius for different coupling scenarios in a DAS only increases the search complexity and therefore it is imperative for a DAS to have an adaptive initial sphere radius to reduce the computational complexity.

To make the sphere radius adaptive, lattice geometry is used to determine the sphere radius [23] for a given number of candidates using the following equation:

$$N_C = \frac{\pi^{\frac{L}{2}} d^L}{\Gamma\left(\frac{L}{2}+1\right) a^L |\det\mathbf{H}|}, \tag{8}$$

where $V_{sphere} = \frac{\pi^{L/2} d^L}{\Gamma(\frac{L}{2}+1)}$ is the volume of the sphere, $V_{unit} = a^L|\det\mathbf{H}|$ is the volume of a single candidate, $L = 2N_T$ is the number of real dimensions, and N_C is the desired number of candidates.

In all of the three scenarios considered, the complexity decreases considerably when the radius is adapted according to users' positions. Although the actual number of candidates is higher than the desired N_c, this number does not increase to a very high value with the reduction in signal coupling. On the other hand, for a static sphere radius at a particular SNR, the number of candidates increases drastically as the coupling decreases, e.g., when the value of radius d is fixed to $\sqrt{3}$ at an SNR of 0 dB, the average number of candidates for FC, PC, and ISO is 14, 110, and 453, respectively. For the adaptive sphere radius at an SNR of 0 dB, d for FC, PC, and ISO is $\sqrt{1.23}$, $\sqrt{0.56}$, and $\sqrt{0.44}$, respectively, and the average number of candidates for FC, PC, and ISO is only 5.11, 6.32, and 7.21, respectively. Thus, by using an adaptive sphere radius there is a substantial reduction in the complexity of SD, and this reduction is most prominent when the coupling is minimum.

The initial sphere radius varies with the channel condition and is therefore a random entity. Its probability distribution not only depends on the fading over the individual links but also on the quality of the channel matrix. Figure 4 shows the probability density function (PDF) of the square of the initial sphere radius d^2 for the FC, PC, and ISO scenarios for $N_C = 2$ and SNR = 4 dB. The PDF plot reveals that the d^2 spread for FC coupled scenarios is much higher, i.e. for good channel conditions, d^2 is as high as seven, while for ill-conditioned channel matrix $\mathbf{H}$, the sphere radius almost approaches zero. The PDFs of the PD and ISO scenarios are dominated by the Rayleigh fading effects of the individual links and have a lower mean and variance than the FC scenario.

5. Simulation results

For simulations, we consider a four-cell DAS with four transmit and receive antennas, i.e. $N_R = N_T = 4$ without loss of generality. The MTs are assumed to be in the FC ($\rho = 1$), PC ($\rho = 1/2$), and ISO ($\rho = 0$) conditions, as explained in Figure 1. The two channels used for the simulation are the i.i.d. Rayleigh channel and the International Telecommunication Union (ITU) vehicular A channel with a bandwidth of 5 MHz and a carrier frequency of 900 MHz. A 1/2 rate parallel concatenated convolution code is used, with each of its component encoders having memory 2 and generator polynomial $(7, 5)_8$. For both QPSK and 16 QAM, gray mapping is employed.

The comparison of SD with ML and linear decoding schemes like ZF and MMSE for the FC scenario is shown in Figure 5. The results show that SD with 32 candidates offers a BER performance approaching the

optimal ML solution at a fraction of the complexity. SD with 32 candidates converges only 0.2 dB after the ML receiver. The comparison of SD with linear schemes shows that SD with 32 candidates converges at 1.3 dB lower SNR than MMSE and 3 dB lower SNR than ZF. SD with a sufficiently large number of candidates offers a good trade off between performance and complexity.

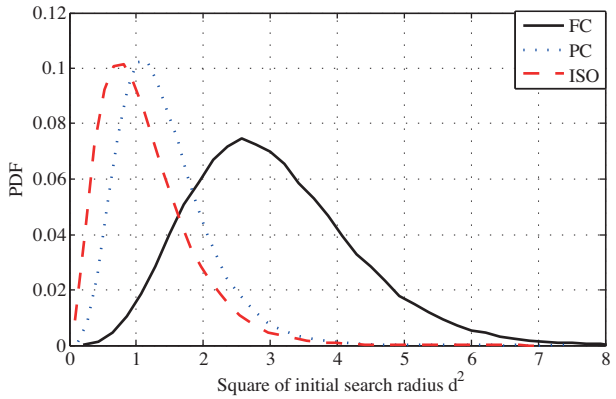

Figure 4. PDF of initial sphere radius for different coupling scenarios: i.i.d. Rayleigh channel, 4 dB, 2 candidates, and 16 QAM.

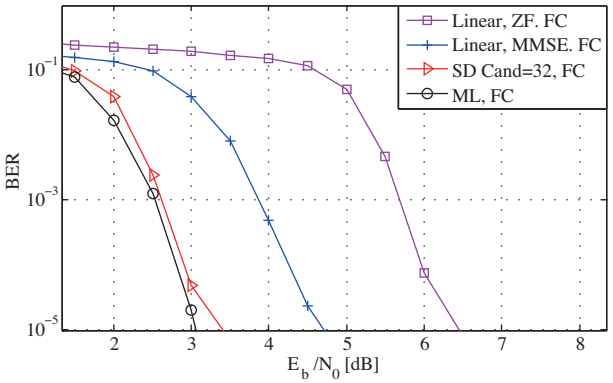

Figure 5. BER performance of SD, ZF, MMSE, and ML: i.i.d. Rayleigh channel, 16 QAM.

The effect of the FC, PC, and ISO cases on the performance of the SD receiver is shown in Figure 6. The channel employed is i.i.d. Rayleigh and both QPSK and 16 QAM are used. In Figure 6a, 2 and 8 candidates are considered and QPSK is used. Here, the FC case converges at a lower SNR due to the increased array and diversity gain. The PC and ISO scenarios have a reduced array gain and thus the convergence takes place at a higher SNR. The resulting 3 dB performance gap between the FC, PC, and ISO scenarios is clearly visible in Figure 6a. The reduction in diversity gain is not perceivable here because of the high diversity inherent within the i.i.d. Rayleigh channel. It can be observed that increasing the number of candidates from 2 to 8 results in a gain of around 2 dB for all of the scenarios. In Figure 6b, the performance of SD for 16 QAM with 8 and 32 candidates is shown. The performance of SD follows the same trend for 16 QAM as for QPSK, i.e. for the same SNR at the local BS the FC scenario outperforms both the PC and ISO scenarios with a difference of

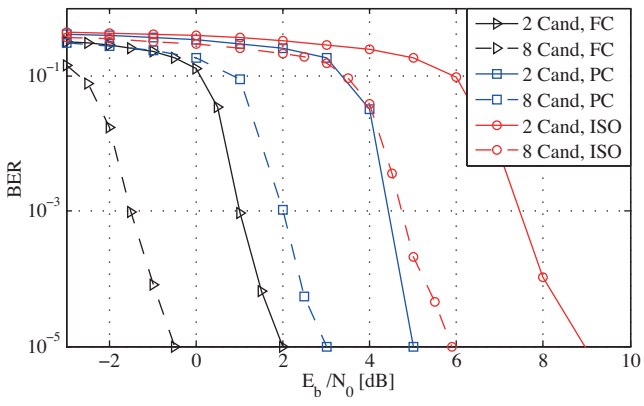

(a) QPSK, N_C=2 and N_C=8.

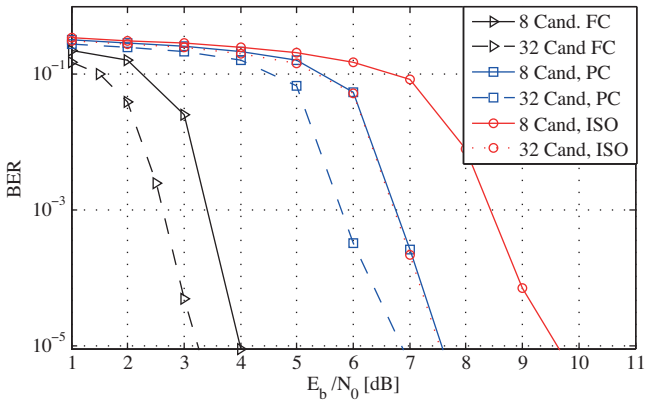

(b) 16 QAM, N_C=8 and N_C=32.

Figure 6. Performance of SD in different coupling scenarios; channel: i.i.d. Rayleigh. a) QPSK, $Nc = 2$ and $Nc = 8$. b) 16 QAM, $Nc = 8$ and $Nc = 32$.

around 3.5 dB between FC and PC and 2 dB between the PC and ISO scenarios. Results show that increasing the number of candidates from 8 to 32 yields a performance gain of between 1 and 2 dB.

With the same simulation parameters as used above, the performance of SD for the ITU vehicular A channel is shown in Figure 7. Figure 7a shows the results for QPSK modulation with 2 and 8 candidates, and Figure 7b shows results for 16 QAM with 8 and 32 candidates. Here, the effect of increased spatial diversity due to multiple streams is more pronounced for the low diversity ITU channel. As expected, the performance of SD improves as the number of candidates increases for different users' positions. Figure 7a shows that increasing the candidates from 2 to 8 results in a performance gain of around 2 dB for all of the scenarios. In Figure 7b, increasing the candidates from 8 to 32 results in a performance gain of only around 1 dB. Because of greater array gain and improved spatial diversity, FC performance converges at a lower SNR than the PC and ISO scenarios.

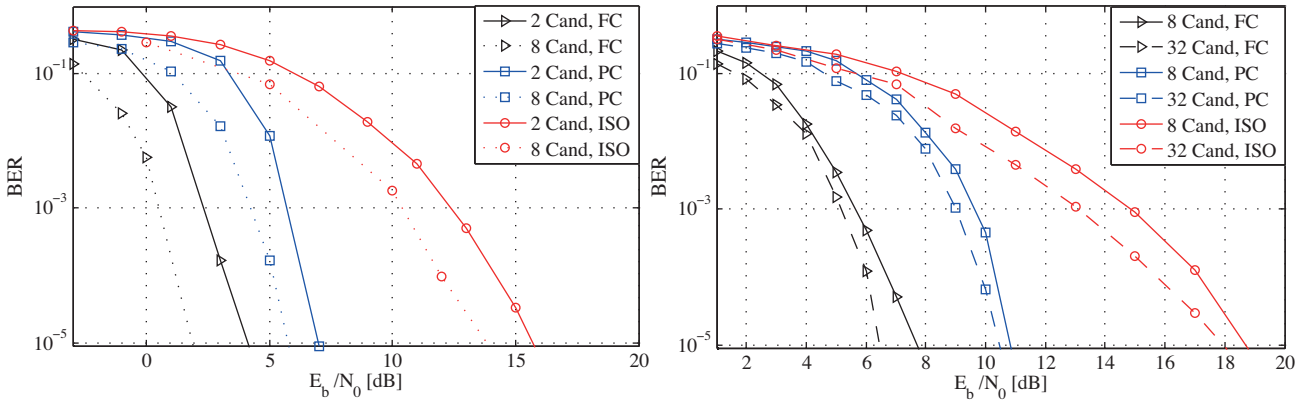

Figure 7. Performance of SD in different coupling scenarios; channel: ITU vehicular A. a) QPSK, $N_c = 2$ and $N_c = 8$. b) 16 QAM, $N_c = 8$ and $N_c = 32$.

6. Conclusion

In this paper, the performance of a multiuser SD receiver in a DAS is investigated for three different symmetric scenarios depending on the users' locations. It can be seen that by increasing the number of candidates the performance of the SD receiver closely approaches that of the ML receiver at a fraction of the complexity. As the channel matrix changes, due to the change in user positions, the SD complexity also varies for a specific initial sphere radius. It is shown that there is a need to have an adaptive initial sphere radius for the different users' positions because using a fixed radius considerably increases the search complexity. An adaptive method for initial sphere radius based on the volume of a $2N_T$ dimensional hypersphere is proposed, which shows promising results. It is shown that the search complexity for the isolated scenario can be improved by an order of magnitude two through this dynamic radius assignment. Additionally, it can be concluded that due to greater array and diversity gain the performance of the users at the cell edge is considerably improved at a given SNR, indicating that a DAS brings about greater benefits for the cell edge users. Conversely, the benefits of the array and diversity gains in a DAS diminish as the users move toward the cell center, indicating that a DAS should be restricted to the cell edge users only.

References

[1] Khattak S, Rave W, Fettweis G. On the impact of user positions on multiuser detection in distributive antenna systems. In: European Wireless Conference; 1–4 April 2007; Paris, France.

[2] Chow P, Karim A, Fung V, Dietrich C. Performance advantages of distributed antennas in indoor wireless communication systems. In: IEEE Vehicular Technology Conference; 8–10 June 1994; Stockholm, Sweden. New York, NY, USA: IEEE. pp. 1522-1526.

[3] Sklavos A, Weber T, Maniatis I, Costa E, Haas H, Schulz E. Interference suppression in multi-user OFDM systems by antenna diversity and joint detection. In: Proceedings of the COST 273 Workshop; 15–17 October 2001; Bologna, Italy.

[4] Khattak S, Rave W, Fettweis G. Multiuser turbo detection in a distributed antenna system. In: 15th IST Mobile & Wireless Communications Summit; 4–8 June 2006; Mykonos, Greece.

[5] Khattak S, Rave W, Fettweis G. SIC based multi-user turbo detector for non gray mapping in distributed antenna systems. In: 9th International Symposium on Wireless Personal Multimedia Communications; 17–20 September 2006; San Diego, CA, USA.

[6] Vikalo H, Hassibi B. On the sphere-decoding algorithm II. Generalizations, second-order statistics, and applications to communications. IEEE T Signal Proces 2005; 53: 2819-2834.

[7] Pohst M. On the computation of lattice vectors of minimal length, successive minima and reduced bases with applications. ACM SIGSAM Bulletin 1981; 15: 37-44.

[8] Viterbo E, Biglieri E. A universal decoding algorithm for lattice codes. In: 14ème Colloque sur le Traitement du Signal et des Images; 13–16 September 1993; Juan-les-Pins, France. pp. 607-610.

[9] Viterbo E, Boutros J. A universal lattice code decoder for fading channels. IEEE T Inform Theory 1999; 45: 1639-1642.

[10] Damen O, Chkeif A, Belfiore JC. Lattice code decoder for space-time codes. IEEE Commun Lett 2000; 4: 161-163.

[11] Fincke U, Pohst M. Improved methods for calculating vectors of short length in a lattice, including a complexity analysis. Math Comput 1985; 44: 463-471.

[12] Schnorr CP, Euchner M. Lattice basis reduction: improved practical algorithms and solving subset sum problems. Math Program 1994; 66: 181-199.

[13] Wubben D, Bohnke R, Kuhn V, Kammeyer KD. MMSE extension of V-BLAST based on sorted QR decomposition. In: Vehicular Technology Conference; 6–9 October 2003; Orlando, FL, USA. New York, NY, USA: IEEE. pp. 508-512.

[14] Zimmermann E, Rave W, Fettweis G. On the complexity of sphere decoding. In: 7th International Conference on Wireless Personal and Multimedia Communications; 12–15 September 2004; Abano Terme, Italy.

[15] El-Khamy M, Medra M, ElKamchouchi HM. Reduced complexity list sphere decoding for MIMO systems. Digit Signal Process 2014; 25: 84-92.

[16] Li LA, de Lamare RC, Burr AG. Successive interference cancellation aided sphere decoder for multi-input multi-output systems. EURASIP J Wirel Comm 2016; 1: 1-16.

[17] Albreem MA, Salleh MF. Radius selection for lattice sphere decoder-based block data transmission systems. Wirel Netw 2016; 22: 655-662.

[18] Khattak S, Rave W, Fettweis G. Distributed iterative multiuser detection through base station cooperation. EURASIP J Wirel Comm 2008; 1: 390489.

[19] Mrinalee S, Garg HP, Mathur G, Yadav RP. Improved radius selection in sphere decoder for MIMO System. In: International Conference on Computing for Sustainable Global Development; 5–7 March 2014; New Delhi, India. New York, NY, USA: IEEE. pp. 161-165.

[20] Shahnaz KV, Ali CK. A sphere decoding algorithm for underdetermined OFDM/SDMA uplink system with an effective radius selection. In: El-Alfy EM, Thampi SM, Takagi H, Piramuthu S, Hanne T, editors. Advances in Intelligent Informatics. Cham, Switzerland: Springer International Publishing, 2015. pp. 169-177.

[21] Babai L. On Lovász' lattice reduction and the nearest lattice point problem. Combinatorica 1986; 6: 1-13.

[22] Hochwald BM, Ten Brink S. Achieving near-capacity on a multiple-antenna channel. IEEE T Comm 2003; 51: 389-399.

[23] Marsch P, Zimmermann E, Fettweis G. Improved methods for search radius estimation in sphere detection based MIMO receivers. In: 14th IST Mobile and Wireless Communications Summit; 29–23 June 2005; Dresden, Germany.